

Color recovery of a chromatic digital image based on estimation of spectral distribution of illumination

Cheol-Hee Lee[†] and Eung-Joo Lee^{**}

ABSTRACT

In this paper, an illuminant estimation algorithm of a chromatic digital image is proposed. The proposed illumination estimation method has two phases.

First, the surface spectral reflectances are recovered. In this case, the surface spectral reflectances recovered are limited to the maximum highlight region (MHR) which is the most achromatic and highly bright region of an image after applying intermediate color constancy process using a modified gray world algorithm. Next, the surface reflectances of the maximum highlight region are estimated using the principal component analysis method along with a set of given Munsell samples.

Second, the spectral distribution of reflected lights of MHR is selected from the spectral database. That is, a color difference is compared between the reflected lights of the MHR and the spectral database that is the set of reflected lights built by the given Munsell samples and a set of illuminants. Then the closest colors from the spectral database are selected.

Finally, the illuminant of an image can be calculated dividing the average spectral distributions of reflected lights of MHR by the average surface reflectances of the MHR.

In order to evaluate the proposed algorithm, experiments with artificial and real captured color-biased scenes were performed and numerical comparison examined. The proposed method was effective in estimating the spectral distribution of the given illuminants under various illuminants.

광원의 분광분포 추정에 기반한 유색 디지털 영상의 색복원

이철희[†] · 이응주^{**}

요 약

본 논문은 유색 디지털 영상을 위한 새로운 광원 추정 방법을 제안한다. 제안된 광원 추정 방법은 두 단계로 나누어 진다. 첫째, 유색 영상의 분광 반사율이 먼저 복원된다. 이때 복원되는 표면 분광 분포는 수정된 그레이 월드 가정을 적용한 영상의 최대 휘도 영역에 제한된다. 다음, 선택된 최대 휘도 영역에 대해 주성분 분석을 통하여 영상의 표면 분광 반사율을 얻는다. 제, 표면 분광 반사율을 구한 후 유색 영상의 최대 휘도 영역에 대한 반사광의 분광 분포를 구한다. 즉 최대 휘도 영역에 해당하는 화소와, 민셀 표색계와 대표 광원의 곱으로 만든 반사광의 분광 분포 사이에 색차 비교를 하여 최대 휘도 영역의 화소와 색차가 가장 적은 반사광의 분광 분포를 찾는다.

최종적으로 최대 휘도 영역의 반사광을 해당하는 표면 분광 반사율으로 나누어 줌으로써 영상에 포함된 유색 광원을 추정한다. 제안된 광원 추정 방법을 평가하기 위하여 인공 유색 영상과 다양한 유색 조명 아래에서 디지털 카메라로 촬영한 실영상에 대하여 광원 추정을 실험하였다. 결과 제안된 광원 추정 방법이 인공 영상과 실 영상, 모두에 대하여 광원의 분광 분포의 추정에 효과적임을 확인하였다.

이 논문은 2000년도 한국학술진흥재단의 지원에 의하여 연구되었음. (KRF-2000-003-E00197)

[†] 정회원, 경운대학교 컴퓨터공학과 전임강사

^{**} 정회원, 동명정보대학교 정보통신공학과 조교수

1. Introduction

The human visual system (HVS) is able to assign roughly constant colors to objects under varying illumination by discounting the illuminants. This adaptability of the HVS enables the accurate identification of objects in diverse visual environments. However, electric cameras have no such adaptation mechanisms, therefore, captured images can exhibit substantial differences according to the incidental light. In order to obtain a similar color appearance for scenes in an electronic camera, illuminant estimation is required so that the stability of surface reflectance can be recovered. This illuminant or surface reflectance decoupling from the reflected colors of scene is called color constancy.

Color constancy in the HVS has been studied by many color-researchers, yet this decoupling process is generally ill-posed problem [1,2]. In the case of a color constancy approach based on a linear model [3], given an RGB-format image including N surfaces, $3N+3$ descriptors are required to decouple an illuminant and surfaces. However, a trichromatic camera system has just $3N$ quantum catch data [2].

As a basic theory in conjunction with a unique recovery for lights and surfaces, D'Zmura and his colleagues presented a criterion for determining this unique recovery according to the number of unknown lights and surfaces parameters based on linear model of Maloney and Wandell [1,3,12]. However, multiple images of a scene with different illuminants are required for exact color recovery. In order to overcome this mismatch between known and unknown descriptors of scenes, additional assumptions have been developed to estimate the surfaces or illuminants of the scenes.

The basic assumption for surfaces is the gray world algorithm that the average spectral reflectance of all the surfaces in the image is gray. Another assumption for surfaces is the brightest surface method, which is one of the most simple

and widely used color constancy algorithms. In this method, the brightest surface of in an image is assumed as a uniform perfect reflector [3]. As a result, the scene illuminant can be decoupled directly.

This paper proposes an effective illuminant estimation method combining the brightest surface method [4] and modified gray world assumption [5]. In order to calculate the brightest surface from color-biased images discounting illuminants, a modified gray world assumption was applied. By using modified gray world assumption, the influence of illumination in the input image is partially eliminated for each channel. Then, the neutralized image is exploited to obtain the maximum highlight region (MHR). After choosing the MHR, the surface spectral reflectances of the MHR are calculated by the principal component analysis [6].

Next, the spectral distributions of reflected lights, which are the closest ones to the colors of the corresponding MHR, are then identified from a set of reflected lights, built by the given set of illuminants and surface reflectances of the Munsell samples. Therefore, color-biased images can be recovered accurately through dividing the spectral power distribution of the reflected lights by the surface spectral reflectance of the MHR.

2. LINEAR MODELS

Linear models have been widely used to approximate three components in the color perception of the HVS. With the use of linear models, illuminants, surface reflectances, and the response of receptors of the HVS can all be represented as weighted sums of basis functions.

$$E(\lambda) \cong \sum_{i=1}^m e_i E_i(\lambda) \quad (1)$$

Where $E_i(\lambda)$ are basis functions used to approximate the spectral measurements of the illuminants, are the illuminant coefficients. Judd collected the spectral power distributions of 622 samples of

daylight to generate 1 mean and 4 basis vectors for the spectral representation of daylight illuminants[7].

Due to smoothness of surface spectral reflectances in the visible wavelength range, a variety of surfaces can be approximated by a fixed set of basis functions, $R_j(\lambda)$ and surface coefficients, r_j as shown below

$$R(\lambda) \cong \sum_{j=1}^n r_j R_j(\lambda). \quad (2)$$

Given an illuminant, $E(\lambda)$ reflected light to a surface with spectral reflectance of $R(\lambda)$ can be represented by the linear models as shown below

$$L(\lambda) \cong \sum_{i=1}^m \sum_{j=1}^n e_i r_j E_i(\lambda) R_j(\lambda). \quad (3)$$

Finally, the quantum catch data caught by the human eye can be represented as photoreceptor responses to reflected lights as shown below

$$q_k \cong \sum_{i=1}^m \sum_{j=1}^n e_i r_j a_{jk}, \quad k=1 \text{ to } p, a_{jk} = \int Q_k(\lambda) E_i(\lambda) R_j(\lambda) d\lambda. \quad (4)$$

Where $E_i(\lambda)$ and $R_j(\lambda)$ are fixed values for input images. Accordingly, color recovery in a trichromatic visual system means decoupling e_i and r_j from the quantum catch data, q_k . However, color recovery in a trichromatic visual system has certain constraints because the number of known parameters is lower than the number of unknown parameters. For a surface, the number of known parameters is 3, yet for an illuminant and surface reflectance 6 coefficients are still unknown. As a result, a direct linear solution to identify the illuminants or surface reflectances using only three quantum catch data is impossible.

To overcome this mismatch, various color constancy algorithms have been introduced including the gray world assumption and the brightest surface method. The former is based on the assumption that the average spectral reflectance of an image is gray, and the latter infers that the brightest surface of an image includes enough information about the illuminant of a scene. This prior infor-

mation on the surface reflectance or illuminants of a scene is then used to recover the remaining illuminants or surface reflectances.

The proposed approach is based on the brightest surface method. However, the conventional brightest surface method cannot recover correctly the illuminant of a scene that has no white points in the image, because, the brightest surface method solves the mismatch on the assumption that white points can estimate illuminants of a scene. As mentioned earlier, the current study is based on the assumption that the brightest region of an image includes sufficient information on the illuminants of a scene. However, we consider that the brightest region in real image cannot be assumed as a uniform reflector. Therefore, our approach can be applied to images without white patches.

In our study, we define the MHR region, which is the maximum highlight region of an image. For MHR, the reflected light and corresponding surface reflectances are calculated. Then, the illuminants of the scene are finally estimated by using the calculated reflected lights and surface reflectances.

3. ESTIMATION METHOD OF ILLUMINANTS OF SCENES

3.1 Estimation of the surface spectral reflectance of MHR

As mentioned before, our approach based on the assumption that if there is a maximum surface reflectance, $R_{\max}(\lambda)$, the maximum spectral power distribution of light reflected from surfaces with an illuminant $E(\lambda)$ will be

$$L_{\max}(\lambda) = E(\lambda) R_{\max}(\lambda). \quad (5)$$

If an image is colorful, the maximum value of the spectral distribution of light reflected from the maximum surface reflectance can be assumed to be an estimation of $L_{\max}(\lambda)$. As a first step, $L_{\max}(\lambda)$ is obtained from the image. Thereafter, the estimation of the illuminant for an input image can

be calculated using the equation below.

$$\hat{E}(\lambda) = \frac{\hat{L}_{\max}(\lambda)}{R_{\max}(\lambda)} \quad (6)$$

Basically, our assumption for equation (5) and (6) is same as in the Cheng's approach [8]. $R_{\max}(\lambda)$ is very important for obtaining an exact description of an illuminant, yet in Cheng's approach, $R_{\max}(\lambda)$ is a fixed value deduced from the assumption that the lights reflected from $R_{\max}(\lambda)$ have a maximum tristimulus value, $q = [111]^T$. Accordingly, $R_{\max}(\lambda)$ is calculated using a fixed spectral distribution of the reflected light with constant weighting vector and fixed spectral distribution of D65.[8] As a result, $R_{\max}(\lambda)$ and the estimated $\hat{E}(\lambda)$ are not adaptive for an image. Plus the estimated $\hat{E}(\lambda)$ cannot be optimal for images that do not include ideal white.

In the proposed method, the $R_{\max}(\lambda)$ and $R_{\max}(\lambda)$ of an image are simultaneously estimated from the same surface of the image. Therefore, the application of the proposed algorithm can extend to images that do not include ideal white because $R_{\max}(\lambda)$ is not required to become a constant spectral function or uniform spectral function.

As the first approach, to identify the MHR, a modified version of the gray world assumption technique of Buchsbaum [9], an intermediate color constancy approach, is applied to partially eliminate the influence of illumination before MHR search.

In equation (7), the average lightness value of each channel indicates the average reflectance at each channel. In the case of illumination variation, the average lightness value of each channel will change.

Hence, normalization using the average of each channel removes the illumination variation and R_{gray} , G_{gray} , and B_{gray} were utilized as the numerators in equation 7, thereby implying a 128 gray value. This is based on the assumption that the average of all the surfaces in an image is that of a middle-gray. Therefore, after applying equation 7, the average of each channel in an image is

mapped to a middle-gray.

$$\begin{bmatrix} R'(i, j) \\ G'(i, j) \\ B'(i, j) \end{bmatrix} = \begin{bmatrix} \frac{R_{gray}}{R_m} & 0 & 0 \\ 0 & \frac{G_{gray}}{G_m} & 0 \\ 0 & 0 & \frac{B_{gray}}{B_m} \end{bmatrix} \begin{bmatrix} R(i, j) \\ G(i, j) \\ B(i, j) \end{bmatrix}, \quad (7)$$

$$R_m = E\{R(i, j)\}, G_m = E\{G(i, j)\}, B_m = E\{B(i, j)\}$$

if $|C_k(i, j) - C_l(i, j)|$ for $k, l = R, G, B$ and $k \neq l > 10$

Where are the color vectors, which have R, G, and B components. When the channel means are calculated for each channel of images, gray colors or dark colors are omitted to avoid saturation of image due to small magnitude of averages in the normalization process. After scaling using the modified gray world assumption, the chromatic images are transformed into $Y C_b C_r$ color space to find MHR as shown below

$$\begin{aligned} Y &= 0.299 R' + 0.587 G' + 0.114 B' \\ C_b &= 0.577 (B' - Y) \\ C_r &= 0.730 (R' - Y). \end{aligned} \quad (8)$$

Then, the MHR is determined by selecting the minimum chromatic points in an image. In equation (9), the local chromatic component, $C(i, j)$, is the linear sum of C_b and C_r in a 7×7 block.

$$\begin{aligned} &\text{if } Y(i, j) > \text{Threshold} \\ C(i, j) &= \sum_{i=1}^7 \sum_{j=1}^7 \sqrt{C_b(i, j)^2 + C_r(i, j)^2} \end{aligned} \quad (9)$$

The 7×7 block size was empirically determined to avoid the selection of impulse noise points in the MHR search. In addition, in order to select bright points, the range of minimum chromatic points is limited to a region where the luminance channel, Y is higher than 90% of that of the input image.

After determining the MHR, the pixels of the central 3×3 block in the selected region are converted into XYZ values in order to apply the principal component analysis method as follows.

$$\begin{bmatrix} X \\ Y \\ Z \end{bmatrix} = \begin{bmatrix} 0.588 & 0.179 & 0.183 \\ 0.290 & 0.606 & 0.105 \\ 0.000 & 0.068 & 1.021 \end{bmatrix} \begin{bmatrix} R \\ G \\ B \end{bmatrix} \quad (10)$$

In order to produce principal components (basis functions) of surface reflectance, 1269 chips from the *Munsell Book of Color* were exploited. The Munsell spectra were obtained from the Information Technology Dept., Lappeenranta Univ. of Tech[10]. Thereafter, three basis functions of these spectra were generated by a principal component analysis.

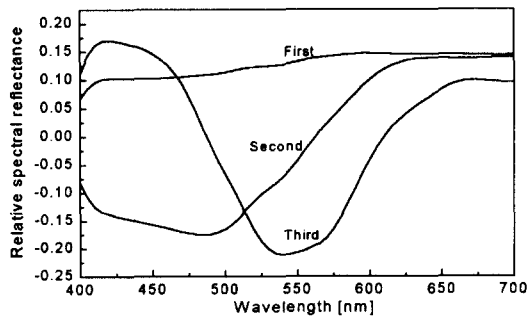


Fig. 1. Principal components for 1269 Munsell chips

Fig. 1 illustrates the three principal components utilized in this study. Using the principal component vectors, the surface spectral reflectances of the object can be expressed as a linear combination as follows

$$\mathbf{R} \cong \bar{\mathbf{R}} + \sum_{i=1}^3 \alpha_i \mathbf{u}_i = \bar{\mathbf{R}} + \begin{bmatrix} \mathbf{u}_1 & \mathbf{u}_2 & \mathbf{u}_3 \end{bmatrix} \begin{bmatrix} \alpha_1 \\ \alpha_2 \\ \alpha_3 \end{bmatrix}. \quad (11)$$

Where, $\bar{\mathbf{R}}$ is the average of surface reflectances. \mathbf{u}_i are the principal components and α_i are the corresponding coefficients to \mathbf{u}_i . In equation (9), the 9 surface coefficients of the selected 9 pixels, that is MHR in an image, can be calculated by equation (12) through (13).

$$\begin{bmatrix} X \\ Y \\ Z \end{bmatrix} \cong \begin{bmatrix} \bar{X} \\ \bar{Y} \\ \bar{Z} \end{bmatrix} + \begin{bmatrix} X_1 & X_2 & X_3 \\ Y_1 & Y_2 & Y_3 \\ Z_1 & Z_2 & Z_3 \end{bmatrix} \begin{bmatrix} \alpha_1 \\ \alpha_2 \\ \alpha_3 \end{bmatrix} \quad (12)$$

Where \bar{X} , \bar{Y} , and \bar{Z} are the tristimulus values

to the averaged spectral of 1269 Munsell samples and X_i , Y_i , and Z_i ($i=1, 2, 3$) are the tristimulus values for the corresponding principal components. Accordingly, surface coefficients are α_i ($i=1, 2, 3$) given by

$$\begin{bmatrix} \alpha_1 \\ \alpha_2 \\ \alpha_3 \end{bmatrix} = \begin{bmatrix} X_1 & X_2 & X_3 \\ Y_1 & Y_2 & Y_3 \\ Z_1 & Z_2 & Z_3 \end{bmatrix}^{-1} \left(\begin{bmatrix} X \\ Y \\ Z \end{bmatrix} - \begin{bmatrix} \bar{X} \\ \bar{Y} \\ \bar{Z} \end{bmatrix} \right) \quad (13)$$

Therefore, the 9 surface reflectances of the MHR can be estimated using above surface coefficients, the spectral mean of Munsell, and principal components as shown in equation (11). Details of principal component analysis along with estimation of surface spectral reflectance can be found in [13].

3.2 Determination of spectral power distributions of the reflected lights on MHR

The proposed approach for estimating the illuminants of a scene has two phases. First, the surface spectral reflectance of the MHR is estimated. Next the spectral distribution of the reflected light of the MHR is determined. In our study, the 1269 samples of *Munsell Book of Color* and 6 illuminants (A, C, D65, D50, Green, Yellow) were used to compose the set of reflected lights. Figure 2 shows the spectral power distributions of the 6 illuminants.

The same 1269 Munsell spectra were utilized for building the principal components for the surface

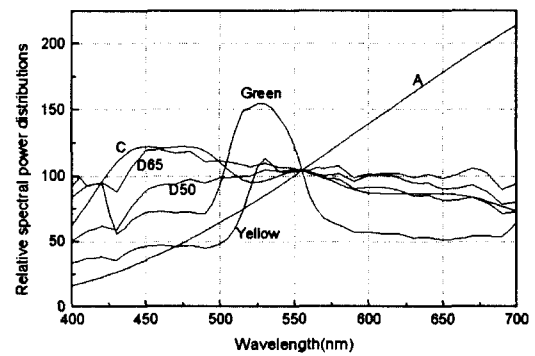


Fig. 2. Spectral power distributions of the 6 illuminants used in constructing the spectral database of the reflected lights.

spectral reflectances and constructing the spectra set of reflected lights. The Munsell spectra were multiplied by 6 illuminants to generate a set of spectral power distributions of reflected lights from 400~700 nm at 5-nm intervals. Hereafter, this set of spectra is referred to as the spectral database. The colors of the MHR are then compared with the spectral database to find the closest spectral data. For a comparison in uniform color space, the 9 colors of the MHR and the spectral data in the spectral database can be transformed into $L^*a^*b^*$ vectors as below :

$$\begin{aligned}
 L^* &= 116f(Y/Y_n) - 16 \\
 a^* &= 500[f(X/X_n) - f(Y/Y_n)] \\
 b^* &= 200[f(Y/Y_n) - f(Z/Z_n)] \\
 f(\omega) &= \begin{cases} \omega^{1/3} & \omega > 0.008856 \\ 7.787\omega + 16/116 & \omega \leq 0.008856 \end{cases} \quad (14)
 \end{aligned}$$

Then, the criterion for selecting the best matching spectra is as follows:

$$\Delta E = \sqrt{(L_{MAR} - L_d)^2 + (a_{MAR} - a_d)^2 + (b_{MAR} - b_d)^2} \quad (15)$$

Where, L_{MAR} denotes the lightness of a MHR color in CIELAB color space and L_d means the lightness of a sample of spectral database in CIELAB metric. Using equation (15), 9 spectral distributions of the lights reflected from the MHR are selected from the spectral database. Finally, the selected spectral data are divided by the corresponding surface spectral reflectances of the MHR and averaged to estimate the spectral distribution of the illuminant. A flowchart of the proposed algorithm is shown in Fig. 3.

3.3 RECOVERING COLORS

After estimating the spectral power distribution of the illuminant, the colors of images with chromatic illuminants can be recovered by matrix transformation. There are three distinct classes of receptors in a trichromatic visual system. Therefore,

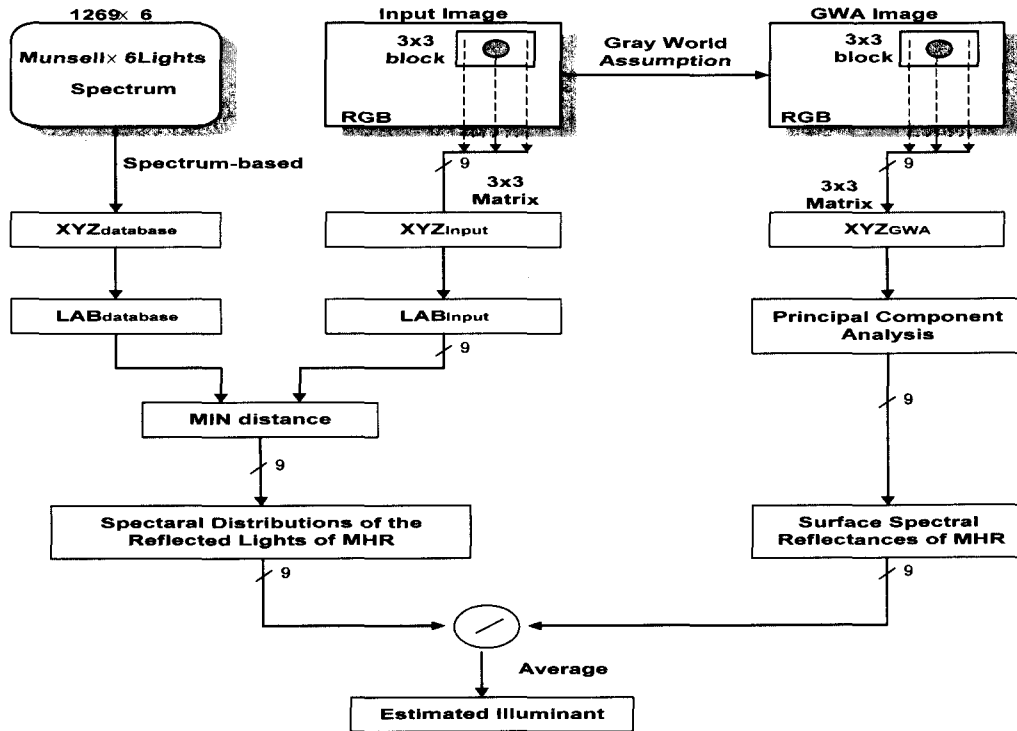


Fig. 3. Flowchart of the proposed algorithm.

the response of a class- k receptor is:

$$q_k = \sum_{j=1}^3 [r_j \int Q_k(\lambda) E(\lambda) R_j(\lambda) d\lambda]. \quad (16)$$

If the illuminant of a scene, $E(\lambda)$ is estimated, the above equation can be expressed in matrix form

$$\begin{bmatrix} X \\ Y \\ Z \end{bmatrix} = \begin{bmatrix} b_{11} & b_{12} & b_{13} \\ b_{21} & b_{22} & b_{23} \\ b_{31} & b_{32} & b_{33} \end{bmatrix} \begin{bmatrix} r_1 \\ r_2 \\ r_3 \end{bmatrix} \quad (17)$$

or

$$\mathbf{q} = \mathbf{B}\mathbf{r} \quad (18)$$

where

$$b_{kj} = \int Q_k(\lambda) E(\lambda) R_j(\lambda) d\lambda. \quad (19)$$

Assume that the column vector of the tristimulus values of a surface with the original illuminant is \mathbf{q}_{orig} and the transformation matrix is \mathbf{B}_{orig} . From the above equation,

$$\mathbf{r} = \mathbf{B}_{\text{orig}}^{-1} \mathbf{q}_{\text{orig}}. \quad (20)$$

Therefore, the recovered image with the CIE standard illuminant D65 can be calculated by

$$\mathbf{q}_{\text{D65}} = \mathbf{B}_{\text{D65}} \mathbf{r} = (\mathbf{B}_{\text{D65}} \mathbf{B}_{\text{orig}}^{-1}) \mathbf{q}_{\text{orig}} \quad (21)$$

Finally, the neutral image in RGB-format can be obtained by an inverse transformation of equation (10) as shown below.

$$\begin{bmatrix} R \\ G \\ B \end{bmatrix} = \begin{bmatrix} 1.971 & -0.549 & -0.297 \\ -0.954 & 1.936 & -0.027 \\ 0.064 & -0.129 & 0.982 \end{bmatrix} \begin{bmatrix} X \\ Y \\ Z \end{bmatrix} \quad (22)$$

4. EXPERIMENT AND DISCUSSION

The proposed method was simulated using artificial color-biased images and digital camera captured images under chromatic light sources. First, to produce artificial color-biased images, the RGB input images were converted to multi-spectral images using linear model and principal components. Here, it was assumed that the scene illuminant of the original image was D65. Then, piecewise multiplication with known chromatic illuminants pro-

duced the artificial color-biased images. A, green, and yellow were utilized as the chromatic illuminants. Each chromatic illuminant has 61 samples and spans 400~700 nm at 5 nm intervals. 1269×6 spectra were used as the spectral database. Fig. 4 through 6 illustrate the results of color recovery and illumination estimation for the artificial color-biased images.

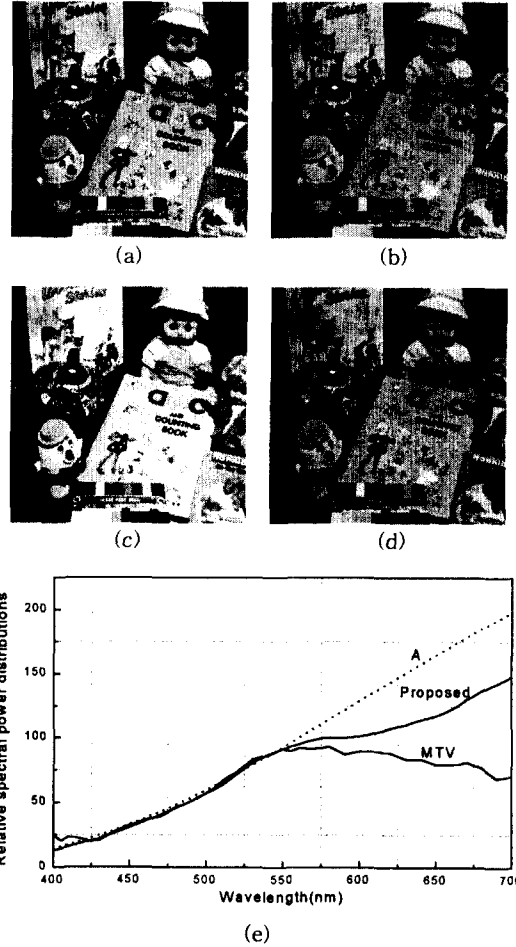


Fig. 4. Recovered images for illuminant A and the spectral power distribution of estimated illuminants.

(a) original image, (b) color-biased image by the illuminant A, (c) recovered image by Cheng's maximum-tristimulus value(MTV) method, (d) recovered image by the proposed method, (e) estimated illuminants A by Cheng's method and proposed method. (dot: original spectral, solid: estimated spectral)

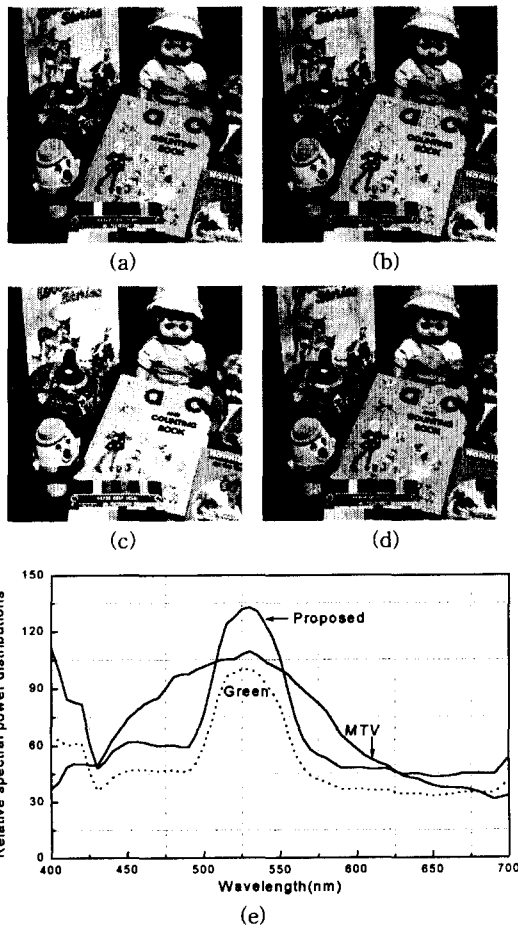


Fig. 5. Recovered images for the green illuminant and the spectral power distribution of estimated illuminants. (a) original image, (b) color-biased image by the illuminant green, (c) recovered image by Cheng's maximum-tristimulus value(MTV) method, (d) recovered image by the proposed method, (e) estimated illuminants green by Cheng's method and by proposed method. (dot: original spectral, solid: estimated spectral)

As shown figure 4 through 6, the illuminants of the artificial color-biased images were then estimated using the proposed and Cheng's *Maximum Tristimulus Value* method. As previously mentioned, in the proposed method, $R_{\max}(\lambda)$ is more adaptive for input images than Cheng's method and does not need to be a constant spectral function or uniform surface spectral function. Therefore, the proposed illuminant estimation method is more

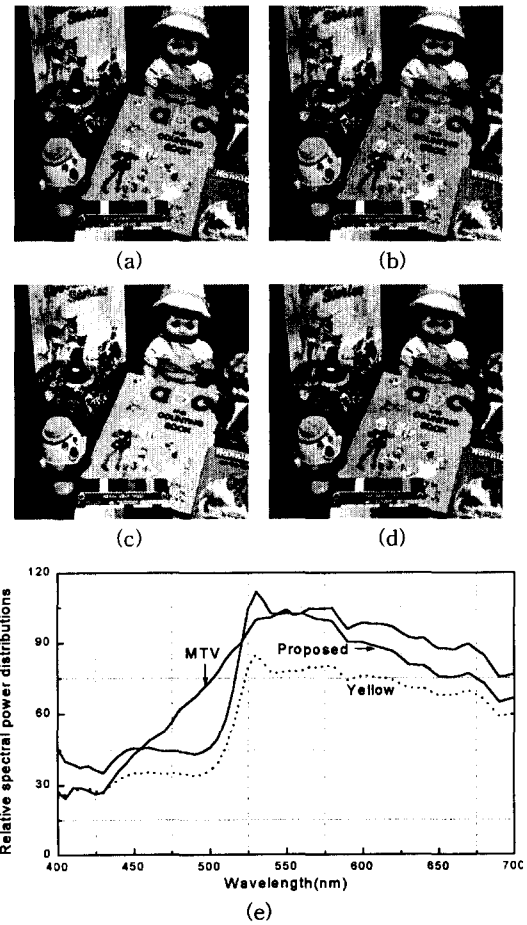


Fig. 6. Recovered images for the illuminant yellow and the spectral power distribution of estimated illuminants. (a) original image, (b) color-biased image by the illuminant yellow, (c) recovered image by Cheng's maximum-tristimulus value(MTV) method, (d) recovered image by the proposed method, (e) estimated illuminants yellow by Cheng's method and by proposed method. (dot: original spectral, solid: estimated spectral)

effective than Cheng's method in illuminant estimation and recovered images also illustrate a better color recovery.

Second, an experiment using real color-biased images was performed. In order to generate the real color-biased images, the *Macbeth Color-Checker* was captured in *Macbeth* viewing booth with changing light sources. A Sony DSC-D700 digital camera was used and its camera-charac-

teristic was fixed to avoid any self-compensation of the scene illuminants. The non-compressed TIFF-format images were converted into RAW-format RGB images using the image manipulation package, Paint Shop Pro 5.0 and then used as the test images.

TL84 and Horizon light sources were utilized as the chromatic light sources in the *Macbeth* viewing booth. Then, the illuminants of the real color-biased images were estimated using the proposed method and Cheng's MTV method and the images were recovered into a neutral image under D65 using the estimated illuminants, respectively. Finally, two resultant images were compared with the captured image under D65 as shown in Fig. 7 and 8.

The results confirmed that the proposed method could effectively estimate the illuminants under different illumination conditions. However, the illuminant estimation for the red-biased image was incorrect in the long wavelength part. As a result, this mismatch was analyzed by investigating the selected spectra in relation to the lights reflected

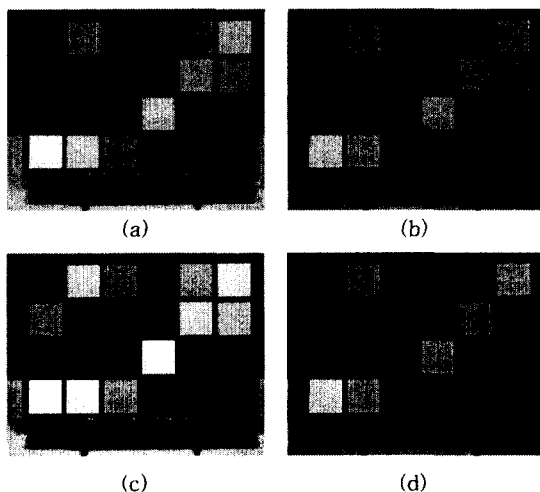


Fig. 7. Experiment for *Macbeth Color-Checker* under Horizon in the *Macbeth* viewing booth. (a) captured image under D65 in the *Macbeth* viewing booth (b) captured image under Horizon light source (c) recovered image by Cheng's MTV method (d) recovered image by the proposed method.

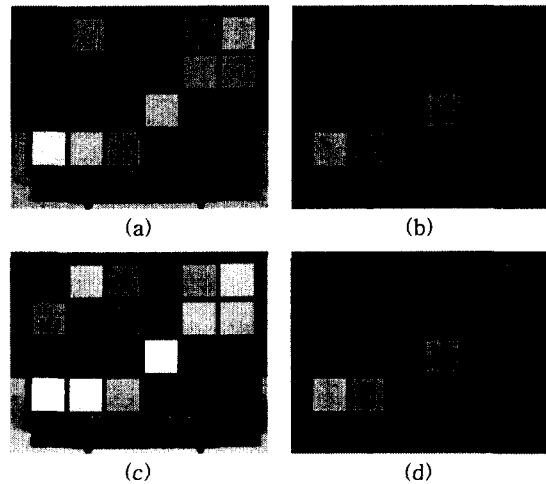


Fig. 8. Experiment for *Macbeth Color-Checker* under TL84 in the *Macbeth* viewing booth. (a) captured image under D65 in the *Macbeth* viewing booth (b) captured image under TL84 light source (c) recovered image by Cheng's MTV method (d) recovered image by the proposed method.

from the MHR. In the case of illuminant A, the selected spectra from the spectral database can include a few reflected lights, illuminated by different lights. Accordingly, the slope in the long wavelength part did not follow the curve of the original illuminant. This phenomenon can be described in three ways.

First, the loss of the red signal when capturing an image can be a reason. An Inc A or Horizon illuminant has a large spectral power distribution in the long wavelength part. Therefore, the captured red signal of an image can exceed the maximum gray level. For reproduction on a monitor, the red signal then should be clipped before saving the image in the camera. Accordingly, a color-biased image caused by Inc A or Horizon will result in lost data in the red channel. As a result, the estimated illuminants will show little difference from the known or the real illuminants in a long wavelength part.

Second, it is a problem related to the dimensional size of the selected minimum color spectra. Namely, 61 dimensional spectral data were represented as the 3-dimensional data of $CIEL^*a^*b^*$. In this proc-

ess, a substantial amount of information on the illuminant color can be lost.

Third, the size of the spectral database also influences the results. A small sample set for reflected lights can create big color differences between the colors of the spectral database. Therefore, if one or two colors, illuminated by different illuminants, are included in the selected spectra, this has a significant influence on the curve of the averaged spectra selected from the spectral database.

In particular, illuminant A is a highly red-biased curve. Accordingly, the sample space between the red-colors in the spectral database includes more void than the sample spaces between other colors. When several spectra were chosen that were illuminated by different illuminants, the error was greater.

Therefore, to improve the accuracy of illuminant estimation, a bigger spectral database for reflected lights is required.

5. CONCLUSIONS

This paper proposed an effective illuminant estimation method combining the brightest surface method and modified gray world assumption. A modified gray world algorithm was adopted to calculate the brightest surface from color-biased images discounting illuminants. The use of the modified gray world assumption enabled the partial elimination of the influence of illumination in the input images for each channel. Thereafter, the neutralized image was exploited to obtain the maximum highlight region (MHR). After determining the MHR, the surface spectral reflectances of the MHR were calculated using a principal component analysis.

Next, the spectral distributions of the reflected lights, the closest ones to the colors of the corresponding MHR, were identified from the spectral database. Then, the color-biased images were re-

covered through dividing the spectral power distribution of the reflected lights by the surface spectral reflectance of the MHR. Finally, the estimated spectral power distributions of the scene illuminants were averaged to generate the illuminant for the input color-biased image.

Based on the results, the proposed method produced good estimations for various illuminants. However, the results of the red-biased image were less accurate, therefore, further research is required to consider the saturation of the red channel in image capture and the size of the spectral database.

An illuminant has a strong influence on determining the color appearance of an object. Therefore, the estimation of the scene illuminant of an image in a spectral domain can be applied to a variety of applications including a color appearance model.

REFERENCES

- [1] L. T. Maloney and B. A. Wandell, Color constancy: A method for recovering surface spectral reflectance, *J. Opt. Soc. Am. A*, vol. 3, pp. 29-33, 1986.
- [2] M. D'Zmura and G. Iverson, Color constancy I. Basic theory of two-stage linear recovery of spectral descriptions for lights and surfaces, *J. Opt. Soc. Am. A*, vol. 10, no. 10, pp. 2148-2165, Oct. 1993.
- [3] B. A. Wandell, *Foundations of vision*, Sinauer Associates Inc., Sunderland, Massachusetts, 1995, pp. 296-308.
- [4] J. J. MaCann, J. A. Hall, and E. H. Land, Color mondrian experiments: The study of average spectral distributions, *J. Opt. Soc. Am., A*, vol. 67, pp. 1380, 1977.
- [5] G. Buchsbaum, A spatial processor model for object color perception, *J. Franklin Inst.* 310, pp. 1-26, 1980.
- [6] M. J. Vhrel and H. J. Trussel, Color correction using principal components, *Color Res. Appl.*

vol. 17, pp. 328-338, 1992.

[7] D. B. Judd, D. L. Macadam, and G. Wyszecki, Spectral distribution of typical daylight as a function of correlated color temperature, J. of Opt. Soc. Am., A, vol. 54, no. 8, pp. 1031-1042, Aug. 1964.

[8] F. H. Cheng, Recovering colors in an image with chromatic illuminant, IEEE Trans. Imaging Processing, vol. 7, No. 11, pp. 1524-1533, 1998.

[9] G. Buchsbaum, A spatial processor model for object color perception, J. Franklin Inst. 310, pp. 1-26, 1980.

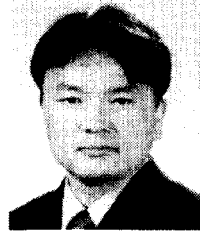
[10] http://www.it.lut.fi/research/color/lutcs_database.html.

[11] E. H. Land, The retinex theory of color perception, Scientific American, 237(6), pp. 108-128, 1977.

[12] M. D'Zmura, Color constancy: Surface color from changing illumination, J. Opt. Soc. Amer. A, vol. 9, pp. 490-493, 1992.

[13] F. H. Imai, *Color reproduction of facial pattern and endoscopic images based on color appearance models*, Chiba Univ. Ph. D. dissertation, pp. 15-18, 1996.

ance models, Chiba Univ. Ph. D. dissertation, pp. 15-18, 1996.



이 철 희

1995년 2월 경북대학교 전자공학과 졸업(공학사)

1997년 2월 경북대학교 대학원 전자공학과 졸업(공학석사)

2000년 8월 경북대학교 대학원 전자공학과 졸업(공학박사)

2000년 3월 ~ 현재 경운대학교 컴퓨터공학과 전임강사

관심분야 : 칼라프린팅, 색채학, 영상처리 등



이 응 주

1992년 2월 경북대학교 대학원 전자공학과 졸업(공학석사)

1996년 8월 경북대학교 대학원 전자공학과 졸업(공학박사)

1992년 3월 ~ 1993년 2월 국방과학연구소 부설 품관소(연구원)

1997년 3월 ~ 현재 동명정보대학교 정보통신공학과 조교수
관심분야 : 영상처리, 컴퓨터비전, 신호처리 등